

Supporting Information For

Reinforced Magnetic Epoxy Nanocomposites with Conductive Polypyrrole Nanocoating on Nanomagnetite as a Coupling Agent

Jiang Guo,^{a,b} Xi Zhang,^{a,b} Hongbo Gu,^a Yiran Wang,^{a,b} Xingru Yan,^{a,b} Daowei Ding,^{a,b} Jun Long,^{a,c} Sruthi Tadakamalla,^a Qiang Wang,^d Mojammel A Khan,^e Jingjing Liu,^f Xin Zhang,^g Brandon L. Weeks,^g Luyi Sun,^f David P. Young,^e Suying Wei^{a,b,*} and Zhanhu Guo^{a,*}

^aIntegrated Composites Lab (ICL), Dan F. Smith Department of Chemical Engineering, Lamar University, Beaumont, TX 77710, USA

^bDepartment of Chemistry and Biochemistry, Lamar University, Beaumont, TX 77710, USA

^cSchool of Chemical engineering and technology, Harbin institute of Technology, Harbin, Heilongjiang 150001, China

^dCollege of Environmental Science and Engineering, Beijing Forestry University, Beijing 100083, China.

^eDepartment of Physics and Astronomy, Louisiana State University, Baton Rouge, LA 70803, USA

^fDepartment of Chemical & Biomolecular Engineering Polymer Program, Institute of Materials Science University of Connecticut, Storrs, CT 06269, USA

^gDepartment of Chemical Engineering, Texas Tech University, Lubbock Texas 79409, USA.

*E-mail: longjun@hit.edu.cn (J. L.); suying.wei@lamar.edu (S.W.); zhanhu.guo@lamar.edu, nanomaterials2000@gmail.com (Z.G.).

Surface functionalization of Fe₃O₄ nanoparticles

Fe₃O₄ nanoparticles were functionalized with PPy via a facile SIP method. Briefly, Fe₃O₄ nanoparticles (4.9510 g), PTSA (15 mmol) and APS (9 mmol) were added into 100 mL deionized water in an ice-water bath for one-hour mechanical stirring (SCILO-GEX OS 20-Pro LCD Digital Overhead stirrer, 300 rpm) combined with sonication (Branson 8510). Then the pyrrole solution (18 mmol in 25 ml deionized water) was mixed with the above Fe₃O₄ nanoparticles suspension and mechanically and ultrasonically stirred continuously for an additional 1.5 hours in an ice-water bath for further polymerization. The product was vacuum filtered and washed with deionized water. The final product was dried at 50 °C overnight. Pure PPy was also fabricated following the aforementioned procedures without adding nanoparticles for comparison.

Characterization of Fe₃O₄ nanoparticles

Fig. S1(a&b) shows the SEM images of the u-Fe₃O₄ and f-Fe₃O₄ nanoparticles. The u-Fe₃O₄ nanoparticles appear as ball-like shape, and the surface of the u-Fe₃O₄ nanoparticles is relatively smooth, Fig. S1(a). However, the surface of the f-Fe₃O₄ nanoparticles becomes much rougher. Fig. S1(c,d,e&f) shows the HRTEM images of the u-Fe₃O₄ and f-Fe₃O₄ nanoparticles. For the u-Fe₃O₄ and f-Fe₃O₄ nanoparticles, the lattice fringes are observed, indicating the highly crystalline structure of the nanoparticles. Compared with u-Fe₃O₄ nanoparticles, the surface of the f-Fe₃O₄ nanoparticles is much rougher, and after functionalization, a thin PPy layer was observed surrounding the nanoparticles and was marked by red cycles. All the results indicate the polymerization of pyrrole occurred on the surface of f-Fe₃O₄ nanoparticles.

The FT-IR analysis is used to verify the surface functional groups. Fig. S1(g) shows the FT-IR spectra of the u-Fe₃O₄ nanoparticles, pure PPy, and f-Fe₃O₄ nanoparticles. In the spectrum of u-

Fe₃O₄ nanoparticles, the only peak at 531 cm⁻¹ is due to the vibration of Fe-O band.¹ For the f-Fe₃O₄ nanoparticles, the peaks at 1536 and 1446 cm⁻¹ are contributed to the C=C and C-N stretching vibration, respectively.² The peaks located at 1288 and 1022 cm⁻¹ are due to the C-H in-plane and out-of-plane deformation vibration, respectively.³ The peak at 1150 cm⁻¹ reflects the vibration of C-C bond.³ The small peak at 957 cm⁻¹ is attributed to the C-C out-of-plane deformation vibration.² All these peaks are the characteristic peaks of PPy in the f-Fe₃O₄ nanoparticles. However, compared with the characteristic peaks of pure PPy, these peaks have some shifts, indicating the interaction between Fe₃O₄ nanoparticles and PPy. All these results show that the Fe₃O₄ nanoparticles have been successful functionalized with PPy.

Fig. S1(h) shows the TGA curves of pure PPy, u-Fe₃O₄ nanoparticles, and f-Fe₃O₄ nanoparticles. For the u-Fe₃O₄ nanoparticles, the weight has only a slight change within the measured temperature. Two weight loss stages are observed in the TGA curves of pure PPy and f-Fe₃O₄ nanoparticles. The weight loss from 30 to 240 °C is attributed to the elimination of the moisture and dopant anions (PTSA).² The major weight loss is due to the decomposition of PPy from 240 to 650 °C.² At high temperature, the Fe₃O₄ nanoparticles are oxidized to form hematite (α-Fe₂O₃). The weight residue of α-Fe₂O₃ is 80.93 % in the f-Fe₃O₄ nanoparticles, then the weight percentage of Fe₃O₄ in the f-Fe₃O₄ nanoparticles is calculated to be 78.23%, which is consistent with the initial 80.0 wt% Fe₃O₄ nanoparticles in the f-Fe₃O₄.

Dispersion quality of epoxy nanosuspensions

Fig. S2 shows the SEM images of the dispersion quality of the f-Fe₃O₄ nanoparticles in the epoxy nanosuspensions. For epoxy nanosuspension with 5.0 wt% of f-Fe₃O₄ nanoparticles, Fig. S2(a), the f-Fe₃O₄ nanoparticles are well dispersed in the epoxy resin. However, when the

particle loading increases to 20.0 wt%, Fig. S2(b), the agglomeration of nanoparticles is obviously observed, which is due to the high particle loading and the magnetic dipole-dipole interactions between the f-Fe₃O₄ nanoparticles.²

Curing degree studied by FT-IR

The curing process of pure epoxy and epoxy PNCs with 10 wt% f-Fe₃O₄ was studied by the FT-IR spectra, Fig. S3. Because the intensity of peak at 913 cm⁻¹ is decreases with increasing the curing extent, therefore, the variation of the epoxy groups can be reflected by this peak. And the absorption peak at 1616 cm⁻¹ of a benzene ring is considered as the internal standard. According to the Beer-Lambert law, the extent of curing (α) is calculated by eqn S1:⁴

$$\alpha = \frac{A_{cured}^{1610} A_{uncured}^{913} - A_{cured}^{913} A_{uncured}^{1610}}{A_{cured}^{1610} A_{uncured}^{913}} \quad (S1)$$

where $A_{uncured}$ is the original absorbance of pure epoxy resin without curing, A_{cured} is the absorbance of cured epoxy and its PNCs. Table S1 shows the curing extent values of pure epoxy and its PNCs with 10.0 wt% Fe₃O₄ nanoparticles. The 0 hour represents the liquid phase samples containing the curing agent, which were heated at 70 °C for about 1-2 hours and were further heated at 120 °C for 5 hours. For the pure epoxy and its PNCs with 10.0 wt% f-Fe₃O₄ nanoparticles, the curing extent increases with increasing the curing time. The curing extent value of the 10.0 wt% f-Fe₃O₄/epoxy PNCs is almost the same as that of pure epoxy, which is due to the reaction between PPy on the f-Fe₃O₄ nanoparticles and epoxide groups. For the 10.0 wt% u-Fe₃O₄/epoxy PNCs, at 0 hour, the curing extent value is even a little higher than that of pure epoxy. However, with increasing the curing time, the curing extent of the 10.0 wt% u-Fe₃O₄/epoxy PNCs becomes much lower, which is induced by the obstructive effect of the nanoparticles.⁴

Differential scanning calorimetry of cured epoxy and its PNCs.

Fig S4. shows the DCS curves of the cured pure epoxy and its PNC with different loadings of Fe₃O₄ nanoparticles. The exothermal peak is observed in all the samples at the temperature range from 150 to 290 °C, indicating that the polymer network in the PNCs is not completely formed during the curing process. As the temperature is above glass transition temperature, the polymer segments can freely move and accomplish the curing process. Therefore, the exothermal peaks are observed. The value of the residual heat during this curing can be used to calculate the curing extent (α) of the PNCs based on eqn S2:⁵

$$\alpha = 1 - \frac{\Delta H}{(1 - W_p)\Delta H_{uc}} \quad (S2)$$

where ΔH is the residual heat during the curing reaction in the PNCs (J/g), W_p is the particle weight percentage in the composites and ΔH_{uc} is the heat of the uncured pure resin (J/g). The ΔH_{uc} value of the uncured pure epoxy is 239.4 J/g. The curing extent (α) are summarized in Table S2. Compared with cured pure epoxy, the α value of the epoxy PNC with u-Fe₃O₄ nanoparticles is a little lower than that of pure epoxy, indicating that the u-Fe₃O₄ nanoparticles can slightly reduce the curing process. However, for the epoxy PNC with f-Fe₃O₄ nanoparticles, the α value is quite different from that of cured pure epoxy, which is induced by the interaction between the PPy on the f-Fe₃O₄ nanoparticles and the epoxide groups. For the epoxy PNC with 5 wt% f-Fe₃O₄ nanoparticles, as the f-Fe₃O₄ nanoparticles is well dispersed in the epoxy matrix, the PPy on the f-Fe₃O₄ nanoparticles can react with the epoxy matrix completely. Therefore the ΔH is increased to 31.11 J/g and the α is decreased to 0.86 as compared with that of the epoxy PNC with 5.0 wt% u-Fe₃O₄ nanoparticles. However, when the f-Fe₃O₄ nanoparticle loading is increased to 10.0 wt%, the agglomeration of nanoparticles occurred which would prevent the

direct interaction between PPy and epoxy matrix, therefore the ΔH is decreased to 20.68 J/g and α is increased to 0.92. With further increasing the particle loading to 20.0 wt%, the agglomeration of the f-Fe₃O₄ nanoparticle is much severe. But there are more PPy reacting with epoxy matrix as compared with the PNC with 5.0 wt% f-Fe₃O₄ nanoparticles. Therefore, the ΔH of the epoxy PNC with 20.0 wt% f-Fe₃O₄ nanoparticles is larger than that of the epoxy PNC with 5.0 wt% f-Fe₃O₄ nanoparticles.

Dielectric property

The dielectric property of the cured epoxy PNCs with different loadings of u-Fe₃O₄ nanoparticles, Fig. S6, is different from that of the cured epoxy PNCs with different loadings of f-Fe₃O₄ nanoparticles. The ϵ' of the cured epoxy PNCs with u-Fe₃O₄ nanoparticles is much lower than that of the cured epoxy PNCs with f-Fe₃O₄ nanoparticles, indicating almost no interfacial polarization occurred. In Fig. S6(a), the ϵ' of the cured epoxy PNCs with 5.0, 10.0 wt% u-Fe₃O₄ nanoparticles has the same trend as that of the cured pure epoxy, and the ϵ' values of the cured pure epoxy and epoxy PNCs with 5.0 and 10.0 wt% u-Fe₃O₄ nanoparticles is almost the same. The ϵ' of the cured epoxy PNCs with 20.0, 30.0 wt% u-Fe₃O₄ nanoparticles decreases with increasing the frequency. At low frequency, the cured epoxy PNCs with 20.0 wt% u-Fe₃O₄ nanoparticles show a higher ϵ' than the cured epoxy PNCs with 30.0 wt% u-Fe₃O₄ nanoparticles. In Fig. S6(b), the ϵ'' of the cured epoxy PNCs with 5.0 and 10.0 wt% u-Fe₃O₄ nanoparticles is almost the same as that of the cured pure epoxy. The cured epoxy PNCs with 20.0 and 30.0 wt% show a higher ϵ'' value. The $\tan \delta$, Fig. S6(c), of the cured epoxy PNCs with 10.0, 20.0 and 30.0 wt% u-Fe₃O₄ nanoparticles is lower than that of the cured epoxy PNCs with 10.0, 20.0 and 30.0 wt% f-Fe₃O₄ nanoparticles, indicating that the cured epoxy PNCs with 10.0, 20.0 and 30.0 wt% u-Fe₃O₄ nanoparticles show a lower dissipation energy.

Table S1. Curing extent value of pure epoxy and 10.0 wt% Fe₃O₄/epoxy PNCs at different curing time.

Curing time	0 hour	4 hour	5 hour
Pure epoxy	0.48	0.73	0.74
10.0 wt% f-Fe ₃ O ₄ /epoxy PNCs	0.47	0.68	0.71
10.0 wt% u-Fe ₃ O ₄ /epoxy PNCs	0.54	0.56	0.63

Table S2. Residual heat of curing, and curing extent of the cured pure epoxy and its PNC with different loadings of Fe₃O₄ nanoparticles.

Samples	ΔH (J/g)	α
cured pure epoxy	14.45	0.94
5.0 wt% f-Fe ₃ O ₄ /epoxy PNCs	31.11	0.86
5.0 wt% u-Fe ₃ O ₄ /epoxy PNCs	20.27	0.91
10.0 wt% f-Fe ₃ O ₄ /epoxy PNCs	19.71	0.90
10.0 wt% u-Fe ₃ O ₄ /epoxy PNCs	16.57	0.92
20.0 wt% f-Fe ₃ O ₄ /epoxy PNCs	41.16	0.79
20.0 wt% u-Fe ₃ O ₄ /epoxy PNCs	14.99	0.92

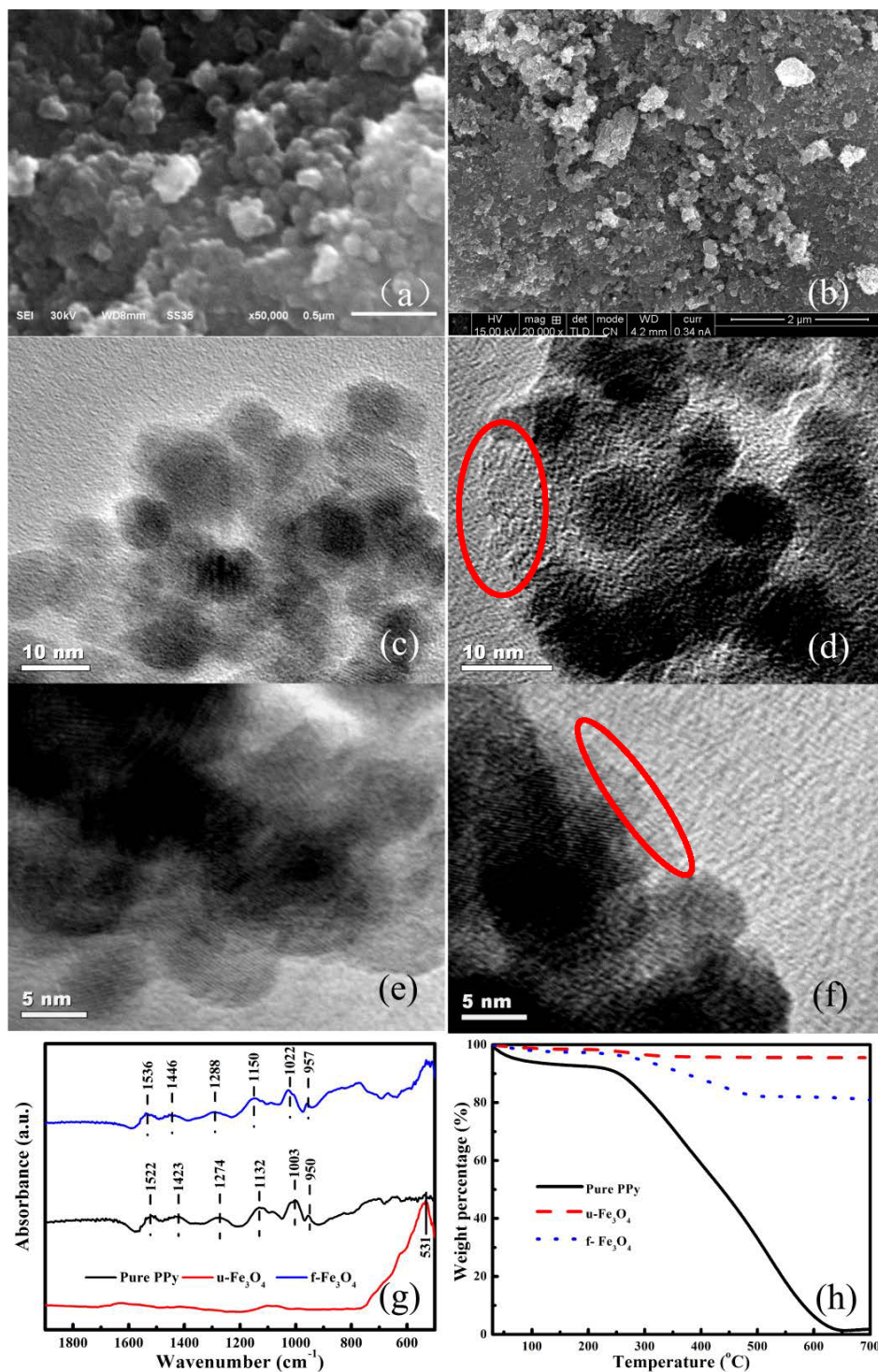


Fig S1. SEM images of (a) u-Fe₃O₄ and (b) f-Fe₃O₄ nanoparticles; HRTEM images of (c,e) u-Fe₃O₄ and (d,f) f-Fe₃O₄ nanoparticles; (g) FT-IR spectra of pure PPy, u-Fe₃O₄ nanoparticles, and f-Fe₃O₄ nanoparticles; and (h) TGA curves of pure PPy, u-Fe₃O₄ nanoparticles, and f-Fe₃O₄ nanoparticles.

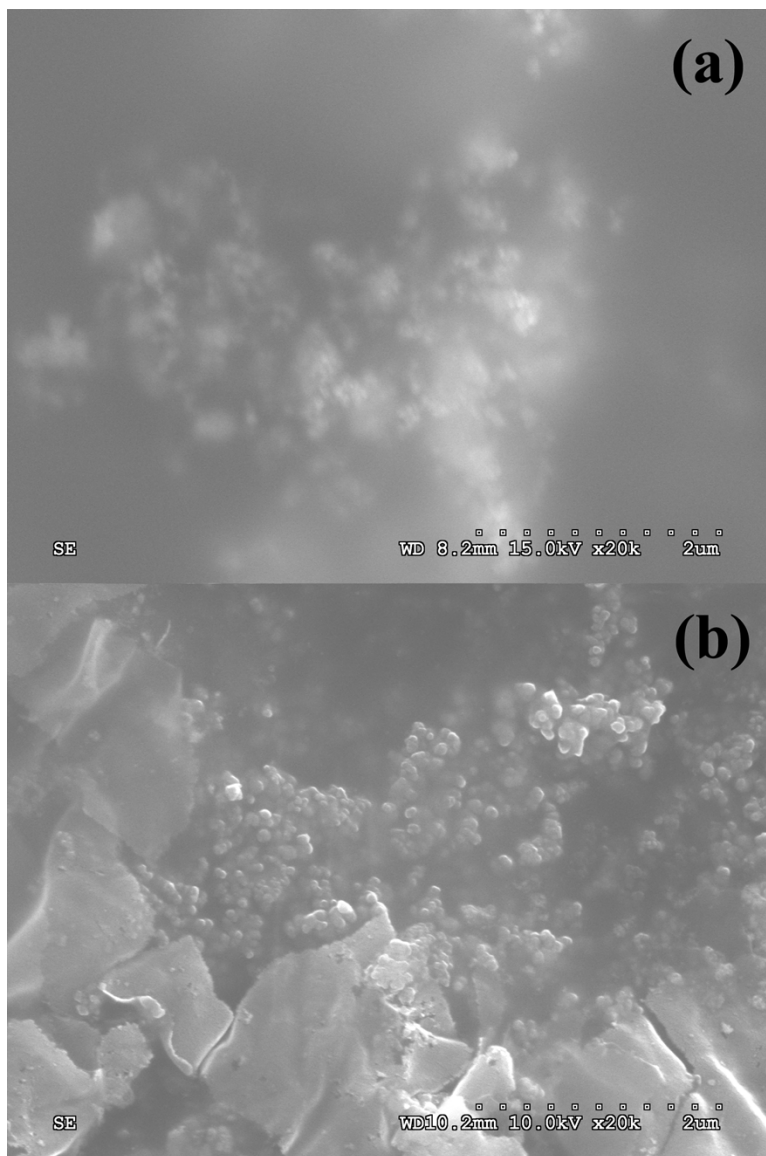


Fig S2. SEM images of the epoxy nanosuspensions with (a) 5.0 and (b) 20.0 wt% of f-Fe₃O₄ nanoparticles.

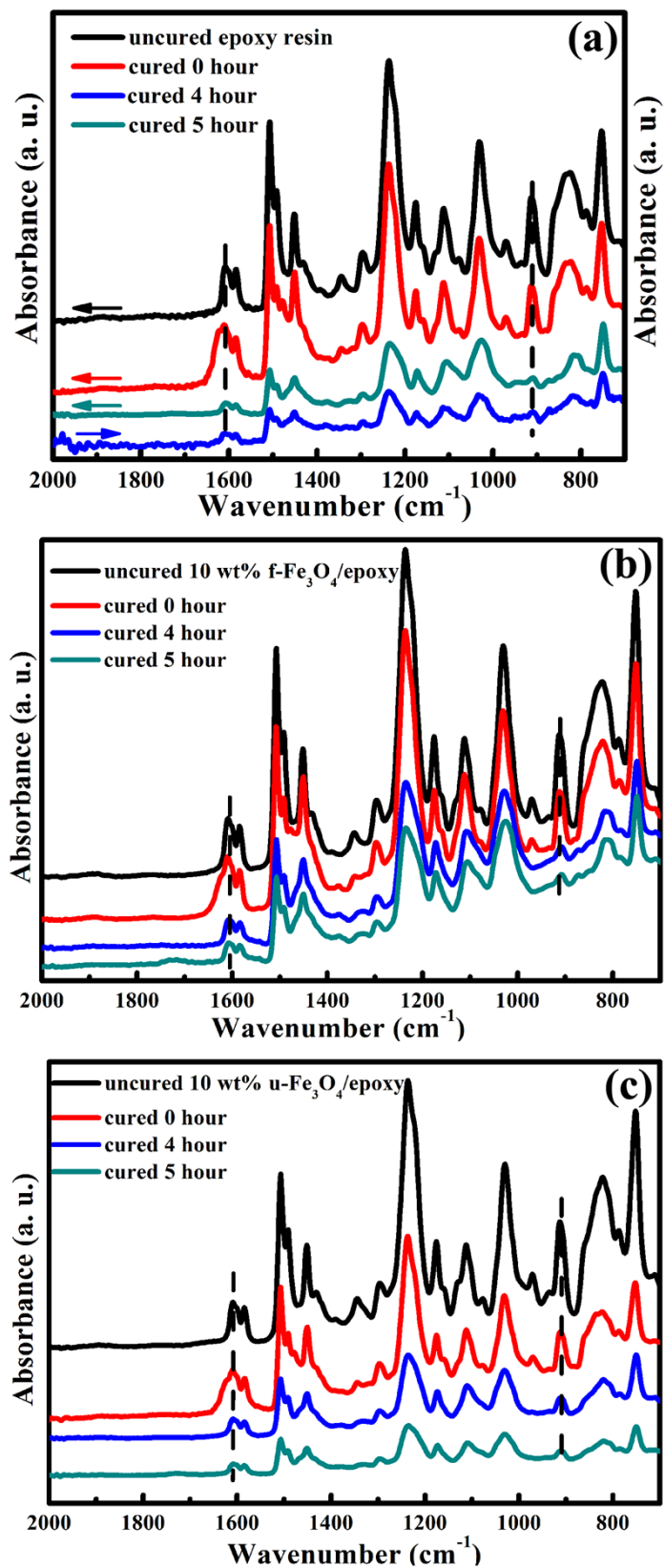


Fig S3. FT-IR spectra of pure epoxy and 10.0 wt% $\text{Fe}_3\text{O}_4/\text{epoxy}$ PNCs.

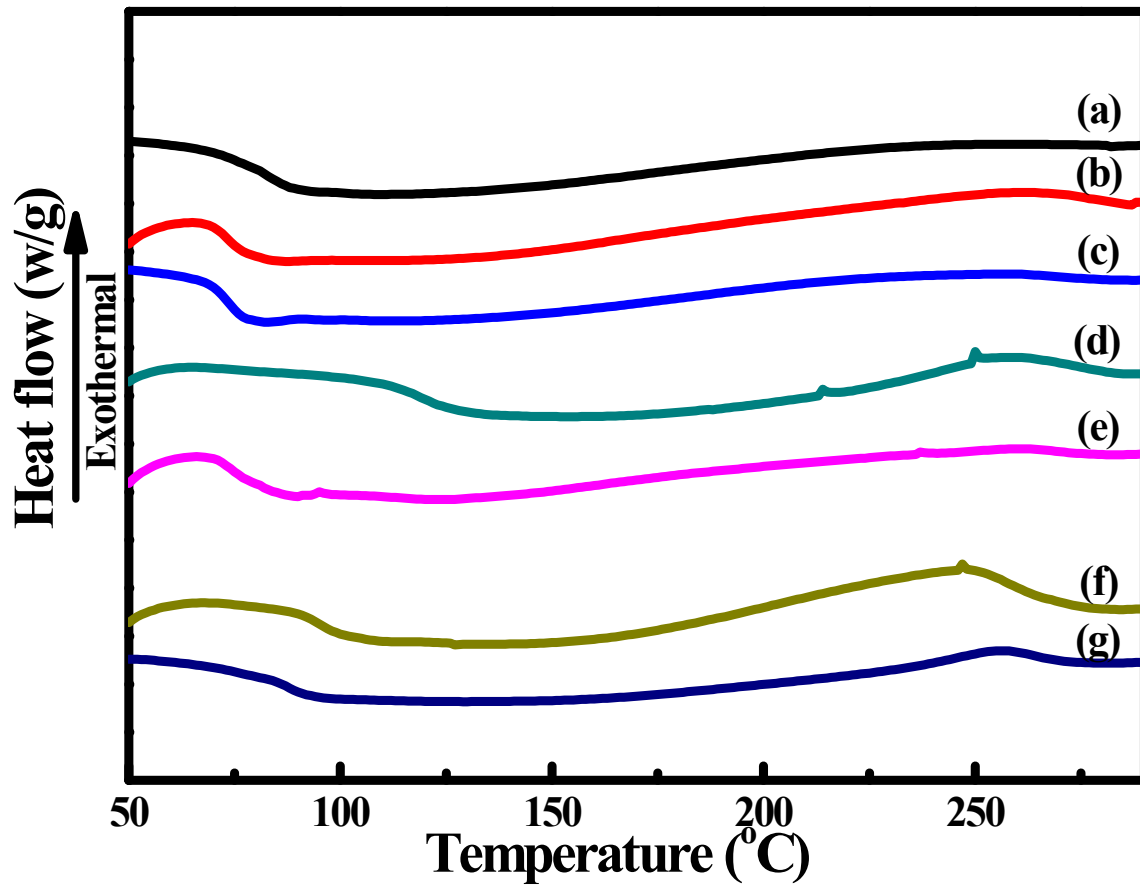


Fig S4. DSC curves of **(a)** cured pure epoxy and epoxy PNCs with **(b)** 5.0, **(d)** 10.0 and **(f)** 20.0 wt% f-Fe₃O₄ nanoparticles; epoxy PNCs with **(c)** 5.0, **(e)** 10.0 and **(g)** 20.0 wt% u-Fe₃O₄ nanoparticles.

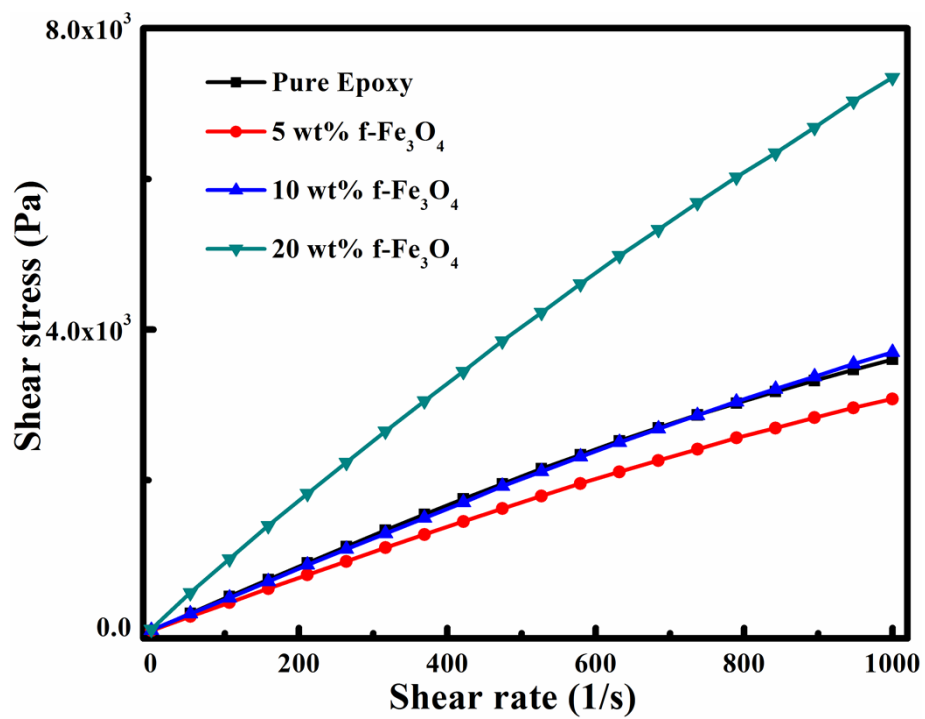


Fig S5. Shear stress vs shear rate of pure epoxy suspension and its nanosuspensions with 5.0, 10.0 and 20.0 wt% f-Fe₃O₄ nanoparticles.

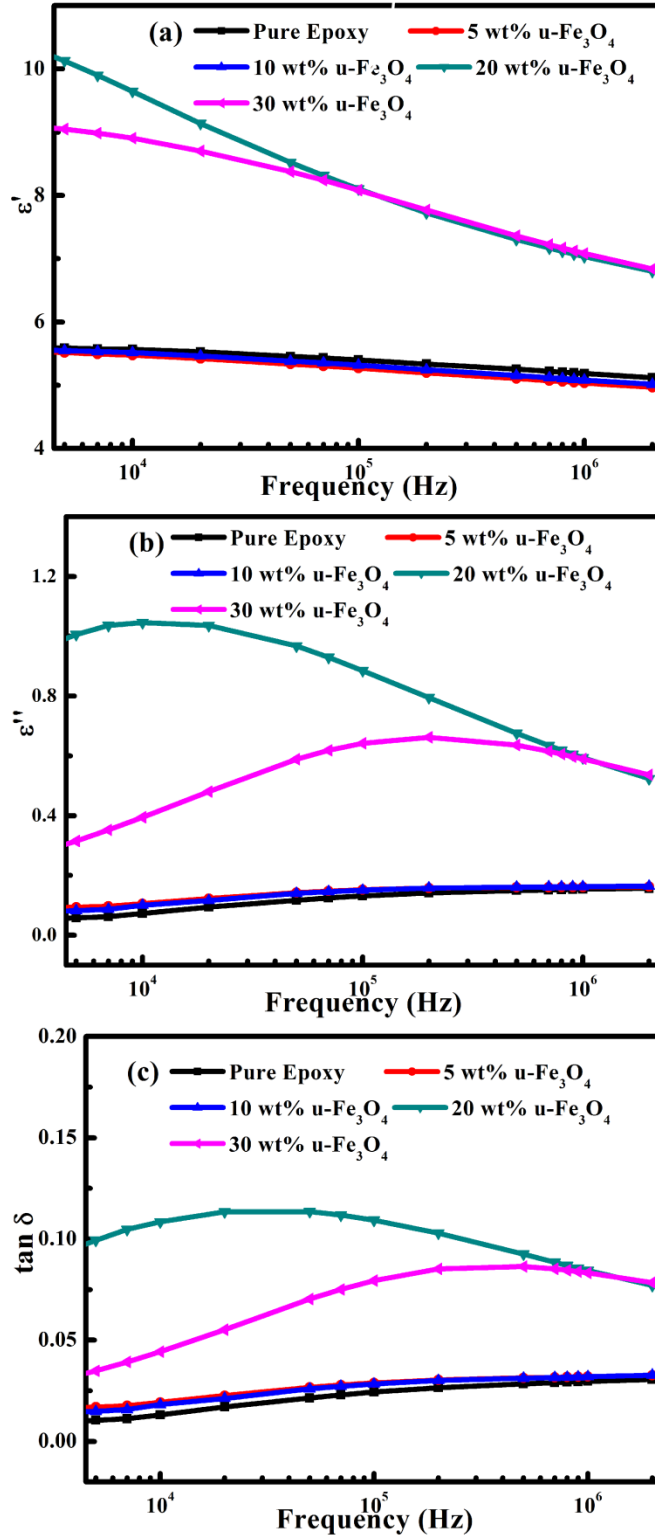


Fig S6. (a) Real permittivity (ϵ'), (b) imaginary permittivity (ϵ''), and (c) dielectric loss tangent ($\tan \delta$) as a function of frequency for the cured pure epoxy and epoxy PNCs with different loadings of u- Fe_3O_4 nanoparticles.

References

1. H. Gu, Y. Huang, X. Zhang, Q. Wang, J. Zhu, L. Shao, N. Haldolaarachchige, D. P. Young, S. Wei and Z. Guo, *Polymer*, 2012, **53**, 801-809.
2. J. Guo, H. Gu, H. Wei, Q. Zhang, N. Haldolaarachchige, Y. Li, D. P. Young, S. Wei and Z. Guo, *J. Phys. Chem. C*, 2013, **117**, 10191-10202.
3. J. Zhu, S. Wei, L. Zhang, Y. Mao, J. Ryu, P. Mavinakuli, A. B. Karki, D. P. Young and Z. Guo, *J. Phys. Chem. C*, 2010, **114**, 16335-16342.
4. X. Zhang, O. Alloul, J. Zhu, Q. He, Z. Luo, H. A. Colorado, N. Haldolaarachchige, D. P. Young, T. D. Shen, S. Wei and Z. Guo, *RSC Adv.*, 2013, **3**, 9453-9464.
5. X. Zhang, O. Alloul, Q. He, J. Zhu, M. J. Verde, Y. Li, S. Wei and Z. Guo, *Polymer*, 2013, **54**, 3594-3604.